Experimental Method for Kinetic Studies of Gas-Solid Reactions: Oxidation of Carbonaceous Matter

Carolin Wang-Hansen, Carl J. Kamp, Magnus Skoglundh, Bengt Andersson, and Per-Anders Carlsson*

Department of Chemical and Biological Engineering and Competence Centre for Catalysis, Chalmers University of Technology, SE-412 96 Göteborg, Sweden

E-mail: per-anders.carlsson@chalmers.se

Abstract

A methodology comprising careful consideration of sample preparation, reactor design, experimental procedures and data evaluation routines for precise analysis of the kinetics of gas-solid reactions, specifically the oxidation of carbonaceous materials, has been developed and validated. The well-controlled solvent-free deposition of the carbonaceous material onto cordierite monolith substrates ensures experimental studies in the absence of diffusion limitations, temperature gradients and hot zones. These critical aspects are supported also by theoretical considerations. Temperature-programmed oxidation and isothermal oxygen step-response experiments in continuous gas-flow reactor using a homogeneous synthetic carbon-black material demonstrate excellent reproducibility and the conversion profiles agree well with previously reported data. An independent set of global kinetic parameters was estimated

---

*To whom correspondence should be addressed

for each 5% sub-conversion interval using linear regression such that the conversion dependence of each parameter could be analyzed separately and compared to previously published data. The results show that the evolution of reactive carbons cannot be described with a single global reaction order. This is supported by intermittent *ex situ* measurements of the specific surface area of the carbon-black material during the course of isothermal oxidation, which reveals a developing microporous structure at high conversions. Physically the changes in carbon reaction order are interpreted as changes in fraction of accessible reactive carbon atoms during progressing oxidation. Moreover, at high conversions, the carbon reaction order approaches 0.7 implying that the evolution of the concentration of reactive carbon atoms is not only proportional to the external surface area of shrinking spheres but also that these spheres have approximately the same size.

Introduction

Studies on the global kinetics of gas-solid reactions, for example oxidation of solid carbonaceous materials, are frequently used to gain insight to the parameters that control the overall reaction rate. During the last three decades, this type of studies has become increasingly more common in the development of technologies for reduction of emissions of particulate matter from automotives[1–8] . To obtain consistent kinetic data is however not straightforward. The main complicating factors are connected to the design of laboratory reactors that operate in regimes without heat- and mass transport limitations,[9–13] inherent variations in carbon reactivity[14,15] and the lack of a unified approach to correct for the changing fraction of reactive carbon atoms during progressive oxidation, i.e. appropriate carbon conversion models.[1,7,16,17]

Studies of gas-solid reactions in the laboratory are often based on the use of packed-bed reactor systems,[18] where the gas flow is either directed through the bed or passed over it. The former have generally a wider experimental window for operation in the pure kinetic regime and it is usually sufficient to dilute the bed with a suitable inert material[1,3,6,8,19] to obtain the kinetically controlled reaction rate. In contrast, packed-bed reactors where the gas flow is passed over the bed typically require careful consideration of mass-transport limitations, originating from, e.g., the stagnant zone often formed between the carbon bed and the gas flow, to be used for kinetic studies. This was brought into notice by, for example, Gilot *et al.*[9] who found it necessary to mathematically compensate for mass-transport effects in the system under consideration to extract reliable kinetic data. The mass transport limitations were assigned to several interacting factors including the design of the sample container, sample size and in specific the sample bed depth as well as the temperature interval, and resulted in several studies on both external[10,20] and internal[21] mass transport. Furthermore, Song *et al.*[13] determined threshold values for the design parameters for sample containers and experimental conditions, which needed to be met to avoid internal- and external mass-transport limitations. Neeft *et al.*[12] studied the influence of heat-transport limitations on the reaction rate and concluded with experimental recommendations.

The inherent reactivity of carbonaceous materials towards oxidation spans a broad range. A higher degree of chemical functionalisation and number of lattice defects generally increase the reactivity.[22] In applications like reduction of soot emissions from automotives (soot is a carbonaceous material), the reactivity of the soot may depend on fuel type,[23] engine load and in-cylinder temperature but also on collection point and sampling technique.[15] All together these variations strongly motivates the use of model substances both for the purpose of method development and as reliable references in reactivity (oxidation) studies. A number of different commercial carbon blacks have been introduced to represent diesel soot, e.g., Printex U (Degussa),[1,4,7,24,25] Hiblack (Degussa),[13] Cabot Vulcan 6 (Cabot),[21] Regal 600 (Cabot),[9] CB-330 (Degussa),[3] 390127-25G (Aldrich),[8] Printex XE-2B (Degussa),[26] Flammruss 101 (Degussa),[26] and FW 1 (Degussa).[22] Furthermore, in-house preparation of soot through the use of a premixed ethylene flame has also been employed.[16,27]

Reactors are for practical reasons often operated in a semi-batch mode, i.e., batch operation with respect to carbon and continuous operation with respect to oxidants. The measured reaction rate must therefore be normalized by a function describing the evolution of reactive carbon atoms in order to obtain a conversion independent estimate of the activation energy and the reaction orders. A number of different methods have been used to find appropriate conversion models. The most common approach is to use an empirical power-law model.[1,2,4,6,7] The power-law model is however often unable to describe the conversion dependence over the entire (0-100%) conversion range.[1,2,4,6,7] The agreement is sometimes unsatisfactory[4] even in the cases where low (< 25%), as well as high (> 80%) conversion stages are omitted.[1,2,4] Models based on more physical mechanisms have also been considered. For example, López-Fonseca *et al.*[8] employed a so-called master-plot method to compare different ideal conversion models with experimentally observed oxidation profiles, and concluded that a mechanism based on surface nucleation and subsequent movement of the oxidation front explained their data most accurately. Furthermore, Neeft *et al.*[4] investigated a pore-growth model but obtained poor agreement with experimental data. In some studies power-law models with a constant carbon reaction order of one[1,7] have been employed or conversion dependencies have been excluded and measured reaction rates have instead been normalized with the initial carbon mass.[16,17,28] In summary, reported kinetic parameters should be interpreted carefully as these may depend on the evaluation procedure, especially on the treatment of eventual conversion dependencies.

The objective of this study is to develop a method for the determination of global kinetics of gas-solid reactions, specifically the oxidation of solid carbonaceous materials. The method comprises careful considerations of sample preparation and reactor design, and procedures for oxidation experiments and data evaluation are established. The method is validated by comparing the characteristics of the oxidation of a well-defined synthetic carbon black with previously published data.

New experimental method

In order to reduce the impact of possible variations in physical- and chemical properties of the solid reactant on the experimental reproducibility, a well-defined commercial carbon black (Printex U, Evonik-Degussa) was used throughout the study. Printex U was introduced first as model substance for diesel soot by Neeft *et al.*[4] and has since then been extensively used by several research groups.[1,4,7,24,25] The morphology and microstructure of Printex U have been considered similar to diesel soot.[29] The average diameter of the primary particles is about 25 nm and the specific surface area as determined by the BET method is approximately 100 m^2/g. Concerning the elemental composition, the carbon content is in the range of 90.5-92.2 wt.-% and the remaining fraction constitutes 8.1-8.4 wt.-% O, 0.52-0.70 wt.-% H, 0.17-0.22 wt.-% N, and 0-0.4 wt.-% S.[19,29,30] Furthermore, Printex U contains negligible amounts of ash or ash forming compounds and the hydrocarbon fraction is in the range 4-5.2 wt.-%.[19,30]

Deposition of Printex U on monolith substrates

In this study ceramic monoliths were used as substrates for distribution of Printex U. Monolith substrates (L=20 mm, ∅=22 mm, 180 channels) were cut out from a commercial honeycomb structure of cordierite(400 cpsi, 6.5 mil) and heated to 650°C in air to remove carbonaceous contaminants. Cordierite, $2MgO \cdot 2Al_2O_3 \cdot 5SiO_2$, is by far the most commonly used ceramic for monolith catalyst support applications.[31] Cordierite undergoes only small dimensional changes due to its low thermal expansion coefficient when cycled over a wide temperature range and can withstand temperatures as high as 1200°C,[32] which makes it a suitable substrate for high temperature kinetic studies. Printex U was uniformly deposited on the walls of the monolith (see Figure 1) by gently shaking the monolith together with approximately 5 ml Printex U in a 30 ml plastic container for 2 min. Excess Printex U was removed by first carefully knocking the monolith against a solid surface and then gently blowing N_2 through the channels. A benefit with this method is that no solvents are used that otherwise may alter the reactivity and thus oxidation kinetics of the solid reactant. To limit the adsorption of water and hydrocarbons from ambient air, the samples were consistently prepared within 10 min before the experiments. About 6 mg of Printex U was deposited on the monolith substrate, which corresponds to approximately 0.8 g/l or a carbon layer with a thickness less than 5 μm assuming even distribution of Printex U on the walls of the monolith substrate. The total amount of Printex U on the monolith substrate could be varied easily by using different amounts of Printex U in the plastic container. As shown in Figure 1a, slightly higher loads can be observed at the inlet- and outlet regions of the monolith substrate. The penetration of Printex U into the cordierite walls is negligible as observed from a microscopic analysis of a wall cross-section.

Consideration of mass- and heat transport limitations

The influence of external mass transfer on the reaction rate can be analyzed by estimating the difference in oxygen concentration between the gas bulk and the surface of the carbon particles using, for example, the so-called film-transport model[33] with the assumption of a reasonable low mass-transfer rate. At stationary conditions, the mass-transfer rate through the fictitious film is equal to the reaction rate, i.e, $r = k_c GSA(c^b_{O_2} - c^s_{O_2})$, where r is the reaction rate, k_c the temperature dependent mass transfer coefficient, GSA the global surface area of the monolith ($2.74 \cdot 10^3$ m^2/m^3), and $c^b_{O_2}$ and $c^s_{O_2}$ the concentration of oxygen in the bulk and at the surface, respectively. The film model is derived for the mass flux towards the entire projected surface, in this case the total surface of the monolith channel. Despite the fact that the monolith surface is not completely covered by Printex U, the distance between the carbon particles is much shorter than the thickness of the fictitious film (see below) so that the same result will be obtained regardless if the analysis is based on surface spots or total surface area. Further, the mass transfer coefficient k_c can be estimated via the Sherwood number (Sh) which equals $k_c d_h / D_{AB}$ where d_h is the hydraulic diameter ($1.105 \cdot 10^{-3}$ m) and D_{AB} the binary diffusion coefficient. Theoretically, the lowest Sherwood number equals d_h/δ where δ is the maximum film thickness ($d_h/2$), which results in $Sh_{min} = 2$. The temperature dependence of D_{AB} can be expressed as $D_{AB} = D_{AB}(T_{ref})(T/T_{ref})^{1.75}$, where $D_{AB}(T_{ref})$ is the binary diffusion coefficient for O_2 at the reference temperature ($0.219 \cdot 10^{-4}$ m^2/s at 298 K). For the most critical conditions in the present study (T=704°C, $C_{O_2} = 0.21$ mole/m^3 and $r_{obs} = 6.4 \cdot 10^{-7}$ mole/s) the concentration difference is $5.9 \cdot 10^{-7}$ mole/m^3, which is negligible in comparison to the O_2 concentration in the bulk and thus external diffusion limitations can be neglected.

To investigate the presence of internal mass transport limitations, i.e., if the reaction between oxygen and carbon is limited by slow diffusion of oxygen inside the carbon spherules, analysis of the so-called Weisz modulus (Φ) can be used. According to Weisz and Prater,[34] internal diffusion will affect a first-order reaction for values of the Weisz modulus equal or higher than one. Conservatively first-order reactions will be kinetically controlled for $\Phi < 0.6$[35] and for reactions with negative reaction orders for $\Phi \geq |n|^{-1}$.[36] The Weisz modulus equals $r_p^2 r_{obs}/(C_{O_2} D_{eff})$, where r_p is the particle diameter, r_{obs} the observed reaction rate, C_{O_2} the concentration of oxygen at the surface and D_{eff} the effective diffusion coefficient. By using a reasonable low value on D_{eff} ($0.7 \cdot 10^{-6}$ m^2/s) and considering the most critical conditions in the present study (T = 704°C, $C_{O_2} = 0.21$ mole/m^3 and $r_{obs} = 38.6$ mole/(m^3s)), the conservative Weisz-Prater criterion is fulfilled for all particles with a diameter less than 60 μm. Although the largest agglomerates may exceed this size, the shape of the agglomerates is not spherical and thus the diffusion distances are generally shorter. In addition the structure is highly porous (*cf.* Figure 1d), except for primary particles, and the overall diffusion is probably significantly higher than assumed here. Therefore internal mass-transfer resistance can be neglected at the present conditions.

The evenly distributed Printex U constitutes only 0.2% of the monolith substrate weight. The monolith substrate therefore acts as heat sink that reduces local temperature gradients during rapid transients. With the present gas flow rate the monolith substrate constitutes at least 50% of the thermal mass for processes shorter than one minute. As the thermal conductivity of the cordierite monolith is 10-20 times higher than for the surrounding gas atmosphere, locally high temperatures, i.e., hot zones, are reduced. Considering an entire (30 min) experiment at the current conditions, where the loaded carbon is completely oxidized, the total mass of the gas passing the sample is almost 20 times higher than the mass of the monolith substrate. In order to obtain a rough estimate of the exothermic temperature increase the average adiabatic temperature increase (ΔT_m) during an oxidation experiment is estimated through the ratio of heat release to thermal mass; $m_C \Delta H_C/(m_{substrate} C_{P,substrate} + \dot{m}_{gas} t C_{p,gas})$, where m_C is the mass of carbon ($6 \cdot 10^{-6}$ kg), ΔH_C the heat of combustion, $m_{substrate}$ and $C_{P,substrate}$ the mass ($3 \cdot 10^{-3}$ kg) and heat capacity (1.05 kJ/(kgK)) of the substrate, $\dot{m}_{gas}$ (0.001 mole/s) the molar flow rate, t the duration of an experiment and $C_{p,gas}$ the heat capacity of the gas mixture (29.12 J/(moleK) for pure N_2). Assuming that the heat of combustion of Printex U is equal to that of graphite (ΔH = 32.76 kJ/g) results in an average temperature increase of about 3°C. This, however, is likely an overestimation given that the heat of combustion for graphite is significantly higher than for Printex U. For example, during the temperature programmed oxidation experiments the measured temperature of the substrate wall equaled the set-point temperature of the inlet gas, and for the isothermal step-response (SR) oxidation experiments the maximum temperature increase ranged between 0.7-2°C (Table 1), which indicates that the reactor is nearly adiabatic. Axial differences in exothermic heat release could not be observed.

Experimental reactor system

The sample was designed as to be used in laboratory continuous gas-flow reactor systems. As the maximum temperature for the present experiments is about 700°C, the reactor was designed to keep axial- and radial temperature gradients small. Briefly, the reactor consists of a horizontal quartz tube (L=700 mm, ∅=22 mm) surrounded by a metal coil for resistive heating, see the schematic cross section of the reactor in Figure 2. The quartz tube and heating coil were insulated by a 100 mm thick layer of carefully wrapped SUPERWOOL 607 HT from Thermal Ceramics. A thermocouple (Reckmann type k) placed in a blank monolith body about 10 mm upstream the sample was used to control the inlet gas temperature via a PID regulator (Eurotherm). The sample temperature was monitored by two thermocouples placed, respectively, in the center and rear part of the monolith sample. Gases were introduced to the reactor via individual mass flow controllers (Bronkhorst Hi-Tech). The CO and CO_2 concentrations in the product stream were measured on-line with individual non-dispersive infrared analyzers (UNOR 6N, Maihak).

Special attention was directed to the temperature profile in the monolith sample. Oxidation of carbonaceous materials with gaseous oxygen generally requires temperatures around 600°C to undergo significant conversion rates. Such high temperatures are often associated with significant heat losses that may cause severe temperature gradients in the sample under consideration and lead to poor correlation between observed oxidation rates and temperature. By mounting bare cordierite monolith bodies, functioning as heat radiation shields, up- and downstream the sample monolith and by carefully considering the insulation thickness, severe temperature gradients were avoided. This was supported by both temperature measurements and quenched oxidation experiments showing an even distribution of remaining Printex U on the walls of the substrate indicating an even oxidation. The axial temperature gradients measured for the isothermal step-response experiments at steady-state conditions prior to oxidation are shown in Table 1. For all experiments performed below 650°C the measured temperature gradients are less than 2°C. Above 650°C, however, somewhat larger gradients were found. Considering the temperature-programmed experiments, the maximum axial temperature difference $T_{center} - T_{rear}$ is about -3°C at 450 °C and +3°C at 750°C. At about 650°C the center- and rear temperatures are equal. In order to consider the influence of these relatively small temperature gradients on the global kinetics, the global activation energies were estimated on the basis of the center- and rear temperatures, respectively, which roughly indicated a 3% difference.

Oxidation of Printex U

Temperature programmed oxidation (TPO) and isothermal step-response (SR) oxidation experiments were carried out to characterize the kinetics of oxidation of Printex U. The obtained results were compared with data reported in the open literature. Generally, TPO experiments provide information about the oxidation process such as the onset oxidation temperature and degree of heterogeneity, i.e., multiple conversion peaks reflect a heterogeneous material while a single smooth conversion profile is indicative of a more homogeneous material.[2] The shape of the TPO profile may also give indications of hot zones through the presence of sharp peaks in the conversion profile[19] as a result of local ignition(s). In contrast isothermal SR oxidation experiments provide qualitative information on changes in reaction kinetics during progressive oxidation. Considering conversion dependencies the same qualitative information can be obtained by a series of either

TPO experiments at different heating rates[8,22] or isothermal SR oxidation experiments at different temperatures.[1–5,16,17] The former may require additional efforts on data processing. The combination of the two experimental techniques can also give complementary information. For example, by comparing the reaction rates obtained with the two techniques at the same temperature and degree of conversion, information on the quality of the experimental results and the heterogeneity of the carbonaceous material can be gained.

The oxidation experiments were conducted at three different levels of oxygen, i.e., 0.5, 2, and 8 vol.-% O_2 (N_2 as balance) with a total gas flow of 1500 ml/min (NTP) corresponding to a space velocity of about 12 000 h^{-1}. The three levels of oxygen reflect typical oxygen concentrations in exhaust gases from diesel- and lean-burn gasoline engines. For the TPO experiments the sample temperature was first increased rapidly from room temperature to 100°C and then linearly increased at a rate of 5°C/min to 750°C. No sample pretreatment was used in order to avoid possible desorption of volatile species[3,16] and restructuring and/or partial gasification of Printex U. The oxygen SR experiments were conducted at three temperatures for each oxygen level. The temperatures were chosen as to achieve detectable amounts of formed CO and CO_2 while also maintaining differential operation. In contrast to the TPO experiments, the SR experiments were conducted with samples that had been pretreated for 10 min in N_2 at 700°C to obtain a consistent initial condition. Experiments conducted at low oxidation rates were finished by complete oxidation of the remaining Printex U at 750°C to close the carbon balance.

Temperature programmed oxidation

The flow-reactor study was started by first ascertain the reproducibility of the experimental procedure. Five TPO experiments with 2 vol.-% O_2 were repeated for slightly different carbon load, i.e., 6.5-7.8 mg as determined from the outlet concentrations of CO and CO_2. As can be seen in Figure 3 the reproducibility is excellent and the difference in carbon load has no significant influence on the oxidation profiles, which also is in line with the theoretical considerations presented above. In Figure 4 the outlet concentrations of CO and CO_2 during TPO with 0.5, 2, and 8 vol.-% O_2 are shown. With increasing oxygen concentration the CO and CO_2 profiles are shifted towards lower temperatures and, due to the Arrhenius type of temperature dependence, also a slight broadening. A similar broadening would occur also for a decrease in heating rate and hence, both the oxygen concentration and heating rate must be considered when comparing experimental data. The present TPO profiles agree reasonably well with those obtained for Printex U by, e.g., Nejar *et al.*[29] using 21 % O_2 and a heating rate of 10°C/min, Setiabudi *et al.*[30] using 10 % O_2 and 0.2°C/min, and 21 % O_2 and 1.5°C/min, and Kalogirou *et al.*[7] using 4.5 and 22 % O_2 and 5, 10, and 20°C/min. The increase of the CO/CO_2 ratio with decreased oxygen concentration, which also is seen in the SR experiments below, is mainly due to the higher activation energy for formation of CO as compared to CO_2[4,16] and thus is a function of temperature rather than oxygen concentration. Furthermore, the circles in Figure 4 show the CO and CO_2 formation rates obtained from the isothermal SR experiments at corresponding temperature and conversion. As can be seen, the oxidation rates agree well with the TPO profiles, which indicates that the oxidation rate is a function of remaining carbon rather than the preceding thermal exposure in these experiments. The fact that nearly the same oxidation rates are obtained in the two different types of experiments can be seen both as a validation of the experimental method and as an indication that Printex U is a homogeneous material.

Isothermal step-response oxidation

Figure 5 shows the CO and CO_2 outlet concentrations for the isothermal SR experiments with 0.5, 2, and 8 vol.-% O_2 at various temperatures (indicated). In all experiments, the oxygen supply is switched on at t=50 s. This results in immediate high formations of CO and CO_2 up to 5-10 wt.-% conversion, which generally is higher for the formation of CO_2 than for CO. Thereafter, at approximately 30% conversion, a second much broader peak can be observed which reflects that the oxidation rate (per carbon) increases significantly, especially as the mass of carbon decreases simultaneously. Finally the measured CO and CO_2 outlet concentrations decrease as carbon is consumed. As mentioned above the higher activation energy for CO formation in comparison to

CO_2 formation[4,16] results in a shift towards higher CO levels at higher temperatures, as shown in Table 1. This is however not observed for the highest temperatures included in our study (673 and 704°C), which may indicate that a small fraction of the formed CO in the primary carbon-oxygen reaction is further oxidized to CO_2 in a secondary reaction at high temperatures. For example, Marcuccilli *et al.*[5] reported an almost 10% conversion of CO to CO_2 at 700°C and a 90% conversion at 800°C.

The high initial reactivity has been noticed previously for diesel soot[4,6,37] and associated with oxidation of highly reactive hydrocarbons[4,6] adsorbed on the carbon surface. However as mentioned by Stanmore *et al.*,[18] adsorbed species tend to desorb before the carbon reaction temperature is reached. Thus a physical- or chemical change of the carbonaceous material might be a more likely explanation. This was suggested by Yezerets *et al.*[37] who found that the initial reactivity could be restored by prolonged exposure to ambient conditions. Considering solid carbonaceous materials generally this phenomenon has been extensively investigated, as it is believed that a relationship exists between the tendency of a solid carbonaceous material to form surface oxide complexes and its reactivity.[38] Two mechanisms, which both depend on temperature and oxygen availability, have been considered. On the one hand the formation of stable or metastable surface complexes by irreversible oxygen adsorption and the other hand a surface restructuring.[38] To further investigate this, an isothermal SR experiment was interrupted repeatedly at about 10 wt.-% conversion increments, whereby the sample was exposed to ambient air over night. As shown in the top panel in Figure 6, peaks in CO formation are clearly observed for each oxidative step. The peak area also seems to correlate with the remaining carbon mass. The corresponding interrupted experiment where the sample instead was kept under nitrogen atmosphere in the flow reactor (middle panel) shows only an initial peak similar to the continuous oxygen SR experiment (bottom panel). These experiments support the suggestion by Yezerets *et al.*,[37] that the peak reactivity upon exposure to ambient air is connected to the formation of reactive solid carbon.

Table 1: Summary of relative CO formation, exothermal temperature increase, maximum axial temperature gradient, carbon mass and maximum O_2 consumption for the isothermal oxygen step-response experiments.

$[O_2]$ /vol.-%	T /°C	$CO/(CO+CO_2)$ /vol.-%	ΔT_{exo} /°C	ΔT_{axial} /°C	m_C /mg	Max O_2 depletion /vol.-%
8	558	52	0.7	0.7	4.7	0.34
	578	56	1.4	0.7	7.1	0.59
	607	59	1.4	2.0	6.8	0.69
2	605	61	1.3	1.5	6.2	3.1
	629	68	1.3	1.5	6.3	1.8
	662	71	2.0	3.3	7.6	3.0
0.5	650	78	1.1	1.8	5.5	2.8
	673	79	1.1	–*	6.3	4.6
	704	79	1.6	4.0	6.6	7.8

*The rear end thermocouple failed.

Analysis of global kinetics

The open literature contains many reports on global kinetics of the oxidation of model- as well as real particulate matter and several strategies to handle, e.g., carbon conversion dependencies (see Introduction). As the evaluation procedure have been shown to influence the values of the kinetic parameters, there is a need for robust methods in general. Here, a strategy for estimating the complete set of kinetic parameters is presented and compared with analogous data from the open literature followed by an interpretation of the observed conversion dependencies in terms of physicochemical mechanisms.

Estimation of global kinetic parameters

Global kinetic parameters were estimated for a power-law model with the general form

$$r = kf(x)C_{O_2}^{n_{O_2}}, \tag{1}$$

where r represents the reaction rate, k is the Arrhenius rate constant $Ae^{-E_a/(RT)}$ where A is the pre-exponential factor, E_a the activation energy, R the gas constant, T the temperature. Moreover, C_{O_2} and n_{O_2} is the concentration and reaction order for oxygen respectively. The function *f(x)* represents the conversion model describing the evolution of reactive carbon atoms with progressing oxidation. For the conversion model an empirical power-law expression was used:

$$f(x) = n_{C,initial}(1-x)^{n_C}, \tag{2}$$

where $n_{C,initial}$ is the amount of carbon at start of the experiment, x is the mole fraction of oxidized carbon, and n_C is the global reaction order with respect to carbon. Low (<10%) and high (>90%) conversion degrees are omitted in order to avoid, respectively, the fraction of highly reactive carbon species and experimental uncertainties associated with measurements of low concentrations. The negligible content of inorganic compounds in Printex U[19,30] suggests that catalytic side-reactions, i.e. catalytic oxidation of CO, may be neglected. However at the two highest temperatures included here (673°C and 704°C) oxidation of CO in a secondary reaction seems to occur as discussed above. Hence, the kinetic parameters are estimated not only for the formation of CO and CO_2 as two parallel reactions but for the overall ($CO+CO_2$) reaction as well. Under the conditions used here, the reactor can be considered to operate in differential mode and the consumption of available oxygen supplied by the feed gas is generally low as shown in Table 1. A minor oxygen concentration gradient may develop only at high reaction rates for the experiments carried out at high temperature with 0.5 vol.-% O_2.

Figure 7 shows the normalized reaction rate ($r_{norm} = r/f(x)$) as a function of conversion obtained for an isothermal SR experiment (558°C and 8 vol.-% O_2) in the case of fixed ($n_C = 1$ and 2/3) and variable carbon reaction orders. In the latter case the values for n_C are obtained by linear regression over 5% sub-conversion intervals. The trend in the r_{norm} reflects the corresponding trend in the rate constant. In principle, for a process with constant oxygen reaction order, it is anticipated that the r_{norm} is a horizontal line. Figure 7 shows that neither a first order dependence nor a shrinking core approximation ($n_C = 2/3$) capture the conversion dependency sufficiently well as indicated by the continuous increase of normalized reaction rate as a function of conversion. For clarity we mention that the shrinking core approximation here alludes to the case where the reaction occurs on the external surface of a sphere, which results in the carbon dependence of 2/3.[2] Although the shrinking core approximation is significantly better, the r_{norm} still increases by more than 50% over a 10-90% conversion interval. We mention that a fixed carbon reaction order of any value cannot completely compensate for the observed conversion dependencies in this study. However, allowing the carbon reaction order to vary between conversion intervals leads to a constant r_{norm} within each interval. With this approach the conversion dependency is captured mainly by the carbon reaction order and only to a minor extent by the pre-exponential factor, thus facilitating in general the analysis of global kinetic parameters.

Dependence on degree of conversion

The mechanisms giving rise to changes of the fraction of reactive carbon atoms may however also lead to changes of the carbon-carbon bond strength (activation energy) and overall reaction kinetics (oxygen reaction order). The four global kinetic parameters (A, E_a, n_C and n_{O_2}) have therefore been estimated simultaneously by linear regression (least squares) using the complete set of data, i.e., nine isothermal SR experiments. Figure 8 shows the conversion dependence for the four parameters, obtained by linear regression over 5 wt.-% conversion intervals. All the kinetic parameters are to various extents dependent on the degree of conversion. The reaction order with respect to carbon shows the most significant dependence. The conversion dependence for the remaining parameters, A, E_a and n_{O_2}, is minor in comparison. The overall activation energy decreases from 140 to 122 kJ/mole, which is similar to the observations by Kalogirou *et al.*[7] To explain a decreasing activation energy with increasing conversion Neeft[19] proposed that the average carbon-carbon bond strength in the graphitic structure might be weakened by the presence of large amounts of electrophilic atoms, i.e. surface oxygen complexes, at high conversion degrees. Most studies however report a single value for the overall activation energy. This value ranges from 105 to 207 kJ/mol[1,3–8,17,27,28] for oxidation of diesel PM and model soots with most values in a more narrow range from 125 to 168 kJ/mole.[1–4,6–8,16,17,27] The current estimate is thus reasonable.

The overall reaction order with respect to oxygen decreases from 0.72 to 0.64 over the 10-90% conversion interval, as can be seen in Figure 8. This can be compared to previous studies reporting values ranging from 0.2 to 1,[1,3,4,6,7,16,17,28] with the majority between 0.7 and 1.[1,3,4,6,7,16] The physical interpretation of the oxygen reaction order in terms of elementary steps is that for a purely desorption limited process at high surface coverage a reaction order of zero is expected, whereas for an adsorption limited process at low coverage a first order reaction is expected. For Printex U, Neeft *et al.*[4] report an oxygen reaction order decreasing from 0.94 to 0.85 (with large standard deviation ±0.09-0.06) over a 60% conversion range. For diesel PM, Darcy *et al.*[6] report that the reaction order with respect to oxygen decreases with conversion while Neeft *et al.*[4] observed the opposite. Yezerets et al.[1] report that such data for diesel PM scatter with a maximum difference of 0.1. Neeft[19] suggests that lower reaction orders may result from a larger fraction of the product being formed by decomposition of surface oxide complexes as opposed to reaction with gas phase species.

As mentioned above, the most significant dependence on conversion is observed for the carbon reaction order. From 10-20% conversion the carbon reaction order is negative indicating a net-formation of reactive carbon atoms. At approximately 30% conversion, the carbon reaction order is nearly zero. This corresponds to a situation where the concentration of reactive atoms does not depend on the degree of conversion. At conversion degrees higher than 30% the reaction order reaches an almost constant positive value of 0.7, which s close to the the fractional order of 2/3. This implies that the evolution of the concentration of reactive carbon atoms is not only proportional to the external surface area of shrinking spheres but also that these spheres have the same size.[39] This indicates that the entire sample has been exposed to the same reaction conditions in terms of temperature and oxygen concentrations, i.e., supports the high experimental quality discussed above and that for conversions above 30%, all primary particles becomes accessible for reaction.

However in addition to the changes observed for the carbon reaction order, the pre-exponential factor changes during progressing oxidation, e.g., from 0.0007 to 0.0013 for the overall reaction. As the pre-exponential factor in a global kinetic model, such as the one used here, lacks a physical meaning (in contrast to models based on physical mechanisms), the interpretation of conversion dependencies may be analogous to the interpretation of carbon reaction order. Based on this approach the trends in the carbon reaction order, especially the sharp increase at about 50% conversion, are enhanced by the changes of the pre-exponential factor (Figure 8). Our results are similar to the results by Neeft *et al.*[4] who observed poor accuracy in the case where low conversion stages were included. Hence, they reported carbon reaction orders close to 2/3 based on data in the 50-95 % conversion interval for O_2 based oxidation of diesel PM.

Evolution of reactive carbon atoms

As discussed in above, the changes in the fraction of reactive carbon during progressing oxidation of Printex U cannot be described by a single global reaction order with respect to carbon mass. This is not entirely surprising considering the complexity of the processes that govern changes in the fraction of reactive carbon. In addition to reaction front movements and nucleation processes that may increase (or decrease) the density of reactive carbon atoms, opening of occluded micropores and other structural changes may as well increase (or decrease) the accessibility to these atoms. It is therefore more accurate to discuss the observed changes in carbon reaction order in terms of *changes in fraction of accessible reactive carbon atoms* instead of just *changes in fraction of reactive carbon atoms*, as pointed out by Neeft *et al.*[4] Thus the change in carbon reaction order that we observe, may be a combination of processes creating (or destructing) reactive atoms and processes enabling (or hindering) oxygen to access already existing reactive atoms. As changes in carbon accessibility are likely connected to changes in surface area, measurements of the surface area during progressing oxidation may provide useful information.

Figure 9 shows repeated measurements of the specific surface area of Printex U deposited on monoliths at various degree of conversion. The surface area of the monolith substrate is about 0.3 m^2/g,[31] which is significantly lower than the surface area of Printex U and was thus neglected. The surface area increases almost linearly from about 200 to 2000 m^2/g from 0-75% conversion. Highly reproducible experiments were conducted to verify this (see Figure 9). As the measured specific surface area rapidly approaches the maximum theoretical surface area (2630 m^2/g[40]), the material can be regarded as a microporous solid ($d_{pore} < 2$ nm) at high conversion degrees. As the concept of the BET method is not applicable to microporous solids, the generally accepted mechanism is instead pore condensation.[41] Thus, the development of the specific surface area shown in Figure 9 should rather be interpreted in terms of internal pore volume. Regarding results from similar measurements performed by other groups, Yezerets *et al.*[1] also observed a linear increase in specific surface area during conversion for Printex U using 5% oxygen at 400°C, although quantitative differences exist. López-Fonseca *et al.*[8] measured an increase in specific surface area from 80 to 500 m^2 over an 80% conversion range for a model soot (390127-25G from Aldrich). Similar specific surface area for diesel soot, about 300-400 m^2/g at high conversions, as for model soots were found by Ishiguro *et al.*[42] and Yezerets *et al.*,[1] and prior to oxidation but after sample degassing at 600°C by Ahlström *et al.*[28] Gilot *et al.*[10] carried out similar experiments with a synthetic carbon black (Regal 600, Cabot) at different levels of conversion and oxidation temperature but connected the results more to the combustion regimes than the evolution of accessible reactive atoms.

Concluding discussion

Hitherto, we have shown that the development of a method for determining global kinetics of gas-solid reactions and in specific oxidation of solid carbonaceous materials, requires not only deep understanding of the complex oxidation processes but also careful consideration of sample preparation and reactor design, and the procedures to carry out oxidation experiments and data evaluation. In the forthcoming section these aspects are discussed in more detail and general conclusions are made.

The sample preparation route presented here is designed as to avoid the usage of solvents that may alter the oxidation kinetics and to create a situation where diffusion limitations, hot zones and temperature gradients are negligible during carbon oxidation experiments. The influence of mass transfer on the reaction rate was estimated theoretically, e.g., the diffusion of oxygen from the gas bulk to the surface of the carbon particles was shown to be significantly faster than the measured reaction rates. It is thus unlikely that external diffusion is limiting in the oxidation experiments. However, the further diffusion of oxidant into the carbonaceous material is more complex. The extensive usage of packed-bed reactors has lead to numerous investigations on oxidant penetration including for example BET surface area measurements,[10] TEM analysis,[43] experimental and theoretical measurements of diffusion rates through packed-beds,[21] and theoretical analysis of carbon reaction orders.[18] Considering the relatively short diffusion distances in the primary particles, complete penetration is predicted even for the smallest (nano-sized) pores where Knudsen and configurational diffusion apply. Contrarily, for agglomerates and especially clusters of several agglomerates, the diffusion distances become significantly longer and diffusion may influence the reaction rate. Here, this issue is effectively avoided by preparing samples with a low and sufficiently well distributed amount of carbonaceous material on a monolith substrate. Theoretical considerations also supported this.

Considering thermal effects, the developed method may generally be sensitive to the type and amount of solid reactant. It has been shown both theoretically and experimentally that under the present reaction conditions, the sample temperature could vary by about 3°C due to exothermal heat release. It is therefore important to carefully consider the carbon load, especially in relation to the reaction rates. The high flow rate of gas and the relatively large mass of cordierite monolith nevertheless result in an experimental situation where local ignition events are effectively avoided. However, admittedly, minimization of temperature gradients is more difficult in this study as the monolith sample is relatively large. Here relatively large refers to the corresponding situation with a packed-bed reactor with the same carbon load. Temperature gradients could be minimized by the use of bare monolith bodies functioning as heat-radiation shields up- and downstream of the sample monolith and careful insulation. As heat losses generally increase with increased temperature, the magnitude of temperature gradients is closely connected to the absolute temperature interval under study. Indirectly this connects also to the choice of oxidant. For example O_2-based oxidation of carbonaceous materials usually occurs at temperatures above 500°C while NO_2-based oxidation starts already around 250°C. With this in mind, the present experimental set-up is thus well suited for studies of oxidation of carbonaceous materials at temperatures common in applications of automotive emission control.

In addition to the evaluation of mass- and heat transport phenomena in the experimental system, various oxidation experiments were carried out to validate the reactor performance. The course of oxidation of a synthetic carbon black was analyzed in relation to well-known aspects of the oxidation kinetics of carbonaceous materials. The observed trends, such as the temperature dependence of the CO/CO_2 ratio and the initial high reactivity during isothermal oxidation, agreed with previous findings in the open literature. Moreover excellent experimental reproducibility was shown. As the experiments were performed using Printex U, which to our knowledge is the most extensively studied synthetic soot, direct quantitative comparisons to published data were made as part of validation. However, because data for experiments performed under the same conditions is rarely found, or because information on experimental conditions is lacking, quantitative comparisons are often demanding and less precise. To circumvent this drawback, global kinetic parameters were estimated and compared with previously reported values, which generally only requires that the experimental conditions are sufficiently similar as to facilitate that the same reaction pathway dominates.

This brings us to another important aspect, *viz.* formulation of a strategy for estimation of global kinetic parameters. As the oxidation rate of a carbonaceous material generally depends on conversion, there is a need for methods for the analyzes of conversion dependencies. Various approaches have been used, which can be divided into two main categories. The first category (Type

I) assumes that changes in isothermal oxidation rate are solely caused by changes in accessible fraction of reactive carbon atoms, while the second category (Type II) also includes the possibility that changes in carbon-carbon bond strength and/or reaction pathway may occur. The goal of the Type I is to find conversion models that produce a constant reaction rate during progressive isothermal oxidation. Hence, a good conversion model should be independent of the remaining kinetic parameters (A, E_a and n_{O_2}). This is, of course, not the case for Type II. In the present study, the Type I approach was used to estimate an independent set of global kinetic parameters for each 5% conversion interval using linear regression. The trend in conversion dependency for each kinetic parameter over the entire conversion interval was thereafter analyzed and associated with suggested physicochemical changes in the carbon structure and/or oxygen occupancy in line with a Type II approach. Even though all the kinetic parameters depend on carbon conversion, the carbon reaction order shows the most significant dependence. The observed changes in oxidation rate during isothermal oxidation are therefore foremost connected to changes in the accessible fraction of reactive carbon atoms. This was also captured to a certain extent by the pre-exponential factor. However, as global models contain no detailed information about reaction mechanisms, it is not relevant to differentiate between mechanisms that cause changes in pre-exponential factor to those of which cause changes in carbon reaction order. The estimated values of the overall activation energy and reaction order with respect to oxygen were compared to values reported in previous studies. The overall average activation energy falls in the lower range of values reported for model- and diesel soots, which is also the case for the overall oxygen reaction order. Although Langmuir kinetics is generally preferred in power-law models designed for broad concentration ranges as used here, Hurt *et al.*[44] found that the broad distributions of the activation energies for desorption- and adsorption processes on carbonaceous materials may lead to persistent power-law behavior over a much wider range than otherwise expected. This may be the reason for that the majority of the reported values lie within a relatively narrow range, 0.7-1.

In summary a new experimental method for the determination of global kinetics of gas-solid reactions, specifically considering oxidation of solid carbonaceous materials has been developed.

The method comprises careful considerations of sample preparation and reactor design, and establish procedures for oxidation experiments and data evaluation. The method is validated by comparing the characteristics of the oxidation of a well-defined synthetic carbon black with previous published data. The aspects addressed here are critical for the analysis of the corresponding kinetics at technically relevant conditions, e.g. at typical automotive exhaust-gas conditions. Moreover, the present method facilitates analysis of automotive samples, e.g. by direct use of the commercial filter substrates, thereby avoiding specialized sampling devices and contamination risks connected with sample handling. The method is suitable also for systems involving catalysts.

Acknowledgement

This study has been performed within an EMFO project in collaboration with Saab Automobile Powertrain AB and the Competence Centre for Catalysis, which is financially supported by Chalmers University of Technology, the Swedish Energy Agency and the member companies: AB Volvo, Volvo Car Corporation, Scania CV AB, Saab Automobile Powertrain AB, Haldor Topsøe A/S and ECAPS AB.

References

(1) Yezeretz, A.; Currier, N. W.; Kim, D. H.; Eadler, H. A.; Epling, W. S.; Peden, C. H. F. *Appl. Catal. B Environ.* **2005**, *61*, 120.

(2) Messerer, A.; Niessner, R.; Pöschl, U. *Carbon* **2006**, *44*, 307.

(3) Ciambelli, P.; D'Amore, M.; Palma, V.; Vaccaro, S. *Catal. Today* **1994**, *99*, 413.

(4) Neeft, J. P. A.; Nijhuis, T. X.; Smakman, E.; Makkee, M.; Moulijn, J. A. *Fuel* **1997**, *76*, 1129.

(5) Marcuccilli, F.; Gilot, P.; Stanmore, B.; Prado, G. *Int. Symp. Comb.* **1994**, *25(1)*, 619.

(6) Darcy, P.; Costa, P. D.; Mellottée, H.; Trichard, J.-M.; Djéga-Mariadassou, G. *Catal. Today* **2007**, *119*, 252.

(7) Kalogirou, M.; Samaras, Z. *J. Therm. Anal. Cal.* **2009**, *98*, 215.

(8) López-Fonseca, R.; Landa, I.; Elizundia, U.; Gutiérrez-Ortiz, M. A.; González-Velasco, J. R. *Chem. Eng. Jour.* **2007**, *129*, 41.

(9) Gilot, P.; Brillard, A.; Stanmore, B. R. *Comb. Flame* **1995**, *102*, 471.

(10) Gilot, P.; Bonnefoy, F.; Marcuccilli, F.; Prado, G. *Comb. Flame* **1993**, *95*, 87.

(11) Stanmore, B. R.; Gilot, P.; Prado, G. *Thermochim. Acta.* **1994**, *240*, 79.

(12) Neeft, J. P. A.; Hoornaert, F.; Makkee, M.; Moulijn, J. A. *Thermochim. Acta* **1996**, *287*, 261.

(13) Song, Q.; He, B.; Yao, Q.; Meng, Z.; Chen, C. *Energy and Fuels* **2006**, *20*, 1895.

(14) van Setten, B. A. A. L.; Schouten, J. M.; Makkee, M.; Moulijn, J. A. *Appl. Catal. B Environ.* **2000**, *28*, 253.

(15) Kittelson, D. B. *J. Aero. Sci.* **1998**, *29*, 575.

(16) Du, Z.; Sarofirm, A. F.; Longwell, J. P.; C.Mims, *Energy and Fuels* **1991**, *5*, 214.

(17) Silva, I. F.; Lobo, L. S. *J. Catal.* **1990**, *126*, 489.

(18) Stanmore, B. R.; Brilhac, J. F.; P.Gilot, *Carbon* **2001**, *39*, 2247.

(19) Neeft, J. P. Ph.D. thesis, Technische Universiteit Delft, 1995.

(20) Stanmore, B. R.; Gilot, P. *Thermochim. Acta* **1995**, *261*, 151.

(21) Brilhac, J. F.; Bensouda, F.; Gilot, P.; Brillard, A.; Stanmore, B. *Carbon* **2000**, *38*, 1011.

(22) Müller, J. O.; Su, D. S.; Jentoft, R. E.; Krönert, J.; Jentoft, F. C.; Schlögl, R. *Catal. Today* **2005**, *102-103*, 259.

(23) Neeft, J. P. A.; Makkee, M.; Moulijn, J. A. *Fuel Proc. Tech.* **1996**, *47*, 1.

(24) Muckenhuber, H.; Grothe, H. *Carbon* **2006**, *44*, 546.

(25) Wal, R. L. V.; Yezerets, A.; Currier, N. W.; Kim, D. H.; Wang, C. M. *Carbon* **2007**, *45*, 70.

(26) López-Fonseca, R.; Landa, I.; Gutièrrez-Otiz, M. A.; González-Velasco, J. R. *Comb. Flame* **2006**, *144*, 398.

(27) Higgins, K. J.; Jung, H.; Kittelson, D. B.; Roberts, J. T.; Zachariah, M. R. *J. Phys. Chem. A* **2002**, *106*, 96.

(28) Ahlström, A. F.; Odenbrand, C. U. I. *Carbon* **1989**, *27*, 475.

(29) Nejar, N.; Makkee, M.; Illán-Gómez, M. J. *Appl. Catal. B Environ.* **2007**, *75*, 11.

(30) Setiabudi, A.; Makkee, M.; Moulijn, J. A. *Appl. Catal. B Environ.* **2004**, *50*, 185.

(31) Heck, R. M.; Farrauto, R. J. *Catalytic Air Pollution Control Commercial Technology*, 2nd ed.; 2002.

(32) Boger, T.; Heibel, A. K.; Sorensen, C. M. *Ind. Eng. Chem. Res.* **2004**, *43(16)*, 4602.

(33) Kapteijn, F. M.; Moulijn, J. A. *Handbook of heterogeneous catalysis*; VCH Verlagsgesellschaft mbH, Wienheim, 1997.

(34) Weisz, P. B.; Prater, C. D. *Adv. Catal.* **1954**, *6*, 143.

(35) Weisz, P. B. *Z. Physik. Chem., Neue Folge* **1957**, *11*, 1.

(36) Mears, D. E. *Ind. Eng. Chem. Proc. Des. Dev.* **1971**, *10(4)*, 541.

(37) Yezerets, A.; Currier, N. W.; Eadler, H. A.; Suresh, A.; Madden, P. F.; Branigin, M. A. *Catal. Today* **2003**, *88*, 17.

(38) Lear, A. E.; Brown, T. C.; Haynes, B. S. *Int. Symp. Comb.* **1991**, *23*, 1191.

(39) Zhdanov, V. P.; Carlsson, P.-A.; Kasemo, B. *Chem. Phys. Lett* **2008**, *454*, 341.

(40) Peigney, A.; Laurent, C.; Flahaut, E.; Basca, R. R.; Rousset, A. *Carbon* **2001**, *39*, 507.

(41) Freeman, J. J.; McLeod, A. I. *Fuel* **1983**, *62*, 1090.

(42) Ishiguro, T.; Suzuki, N.; Fujitani, Y.; Morimoto, H. *Comb. Flame* **1991**, *85*, 1.

(43) Simonsen, S. B.; Dahl, S.; Johnson, E.; Helveg, S. *J. Catal.* **2008**, *255*, 1.

(44) Hurt, R. H.; Haynes, B. S. *Proc. Comb. Inst.* **2005**, *30*, 2161.

Figures

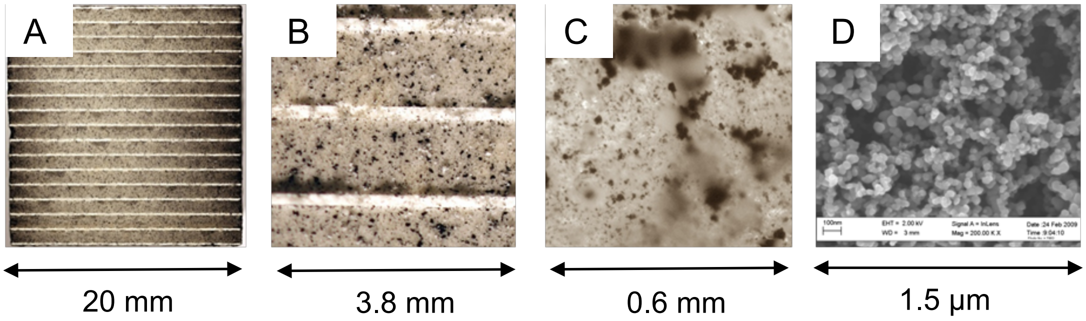

Figure 1: Images of the distribution of Printex U on a standard cordierite substrate. A single-lens reflex camera was used for images A and B, an optical microscope (Olympus BH2-UMA) for image C, and a scanning electron microscope (Zeiss) at 200 000 times magnification using secondary electrons for image D.

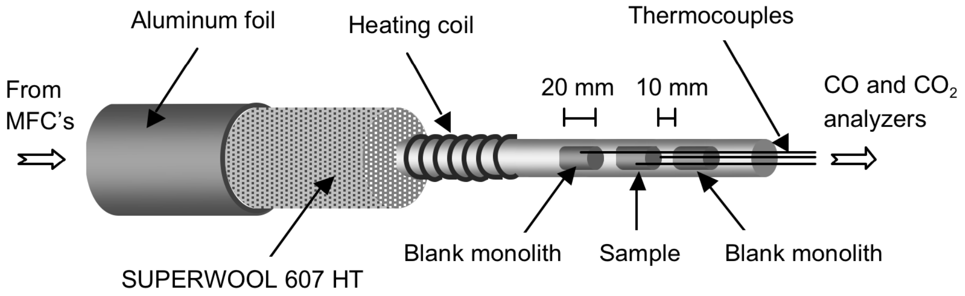

Figure 2: Schematic cross section of the reactor tube. The three monoliths, the sample and the two blank monoliths, are placed on the downstream end of the reactor tube in order to maximize the preheating time for the reactant gas. The heating coil and insulation (glass wool and aluminum foil) covers the full tube length (not shown here).

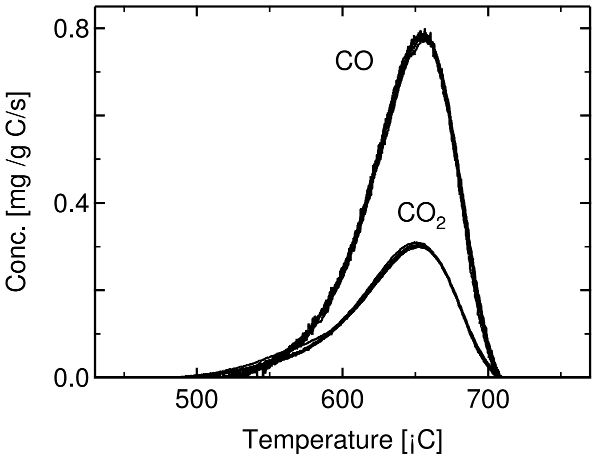

Figure 3: Five repeated temperature programmed oxidation experiments of Printex U (6.5-7.8 mg) deposited on monolith substrates using 2 vol.-% O_2 (N_2 as balance) at a total gas flow of 1500 ml/min and a heating rate of 5°C/min. The figure shows the outlet concentration of CO and CO_2 normalized with the initial carbon load versus monolith substrate temperature for all five experiments.

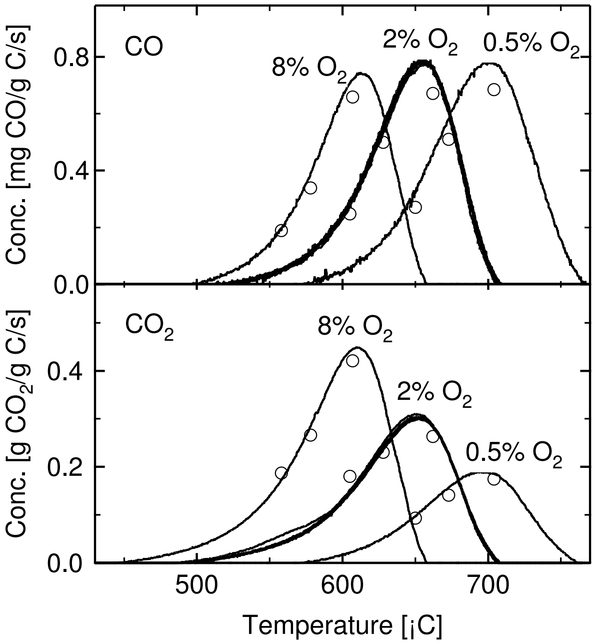

Figure 4: Temperature programmed oxidation of Printex U deposited on monolith substrates using 0.5, 2, and 8 vol.-% O_2 (N_2 as balance) at a total gas flow of 1500 ml/min and a heating rate of 5°C/min. The figure shows the outlet concentration of CO and CO_2 normalized with the initial carbon load versus monolith substrate temperature. Inserted circles indicate the oxidation rates obtained from isothermal step-response experiments at corresponding carbon conversion.

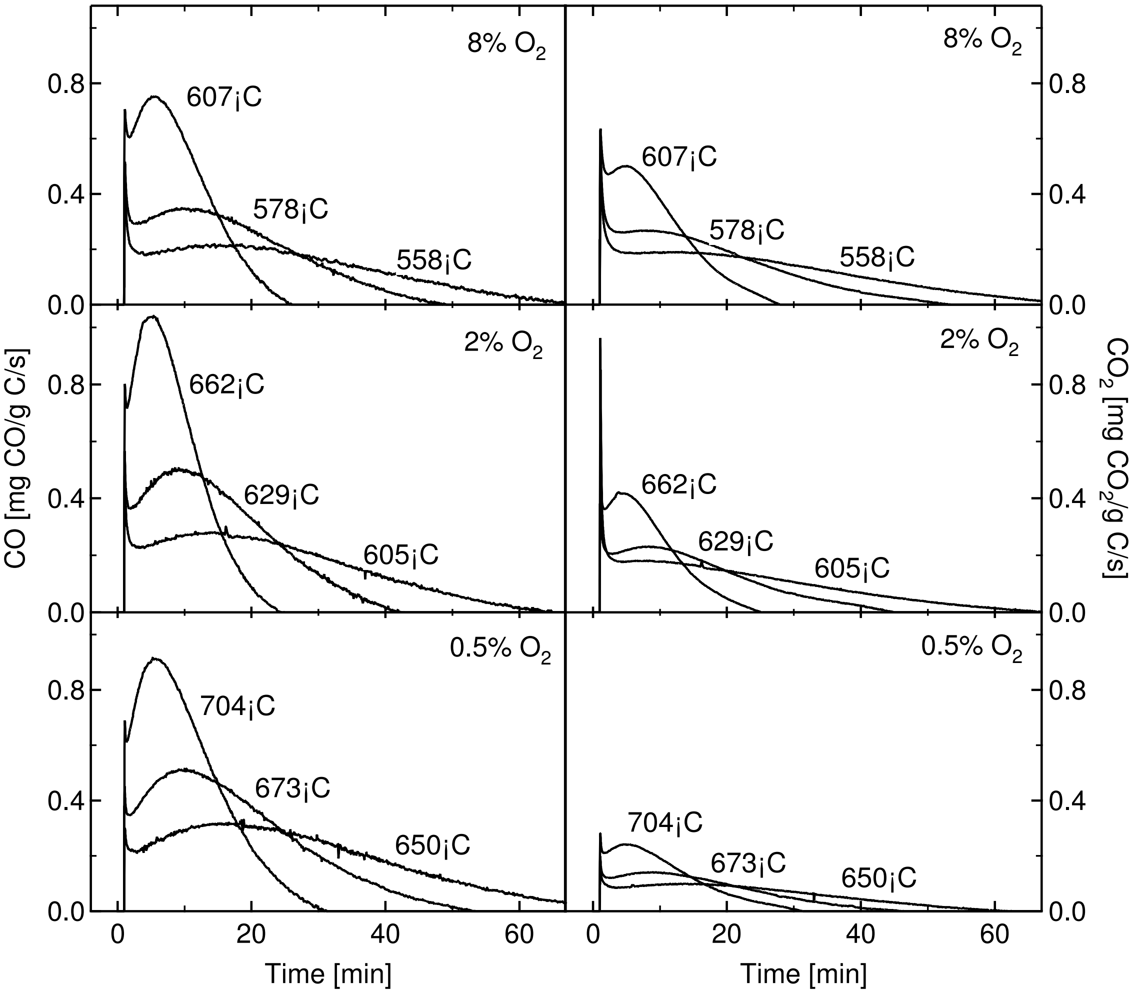

Figure 5: Isothermal step-response experiments of Printex U deposited on monolith substrates using 0.5, 2 and 8 vol.-% O_2 (N_2 as balance) at a total gas flow of 1500 ml/min. The O_2 flow is switched on at t=50s. Three individually selected temperatures for each oxygen concentration were used. The figure shows the on stream outlet concentration of CO and CO_2 normalized with the initial carbon load versus time.

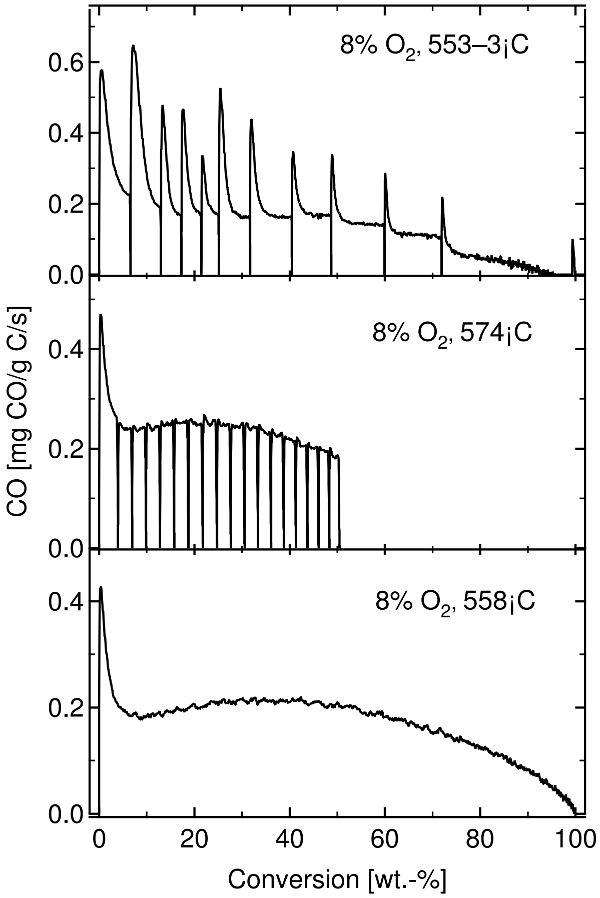

Figure 6: CO formation during SR oxidation with 8 vol.-% O_2; a comparison between experiments were the sample was exposed to ambient air (top panel), pulsing O_2 supply with 60 sec. O_2 and 120 s intervals (middle panel), and continuous O_2 supply (bottom panel).

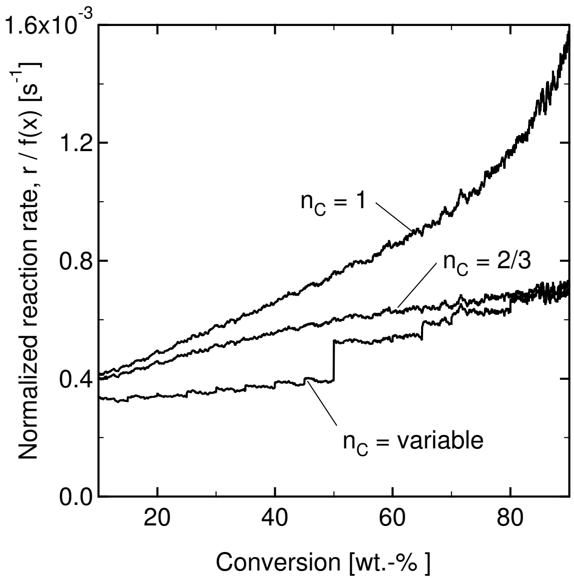

Figure 7: Normalized reaction rate (r_{norm} = *r/f(x)*) as a function of carbon conversion obtained for an isothermal SR oxidation of Printex U at 558°C using 8 vol.-% oxygen in the case of fixed carbon reaction order (n_C = 1 and 2/3) and step-wise variable, i.e., -0.97, -0.67, -0.55, -0.39, -0.25, -0.13, 0.036, 0.050, 0.47, 0.48, 0.51, 0.59, 0.63, 0.62, 0.65, 0.65 obtained by linear regression over 5 wt.-% conversion intervals from 10-90% conversion.

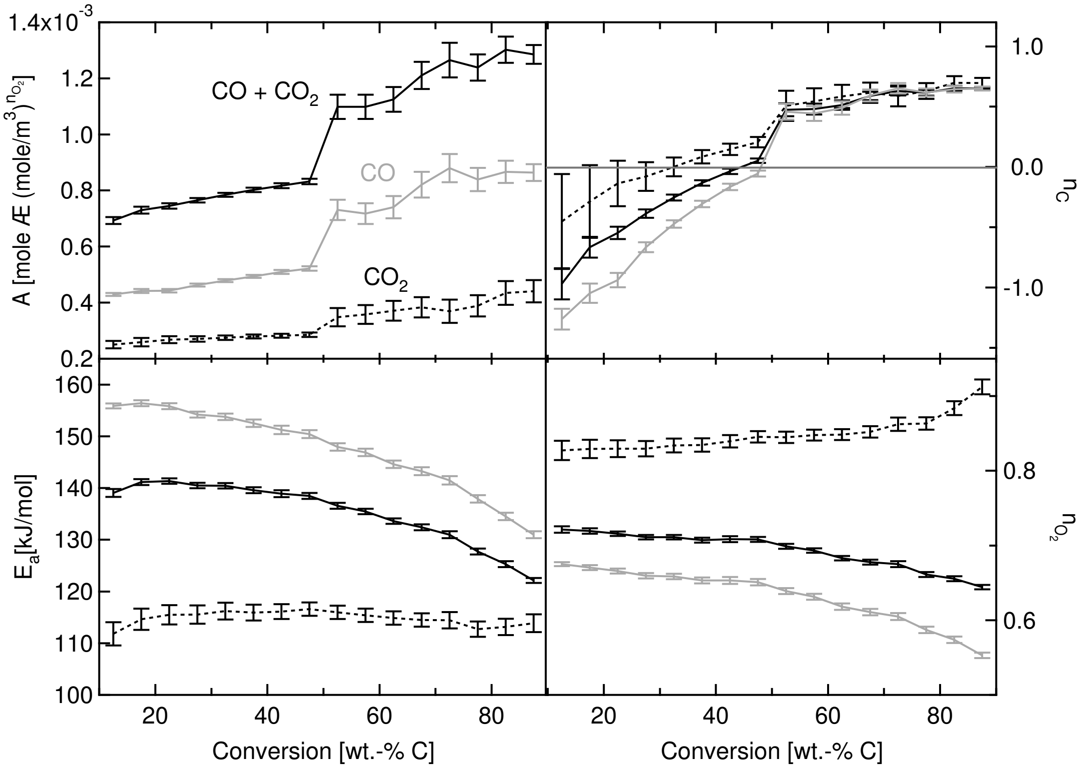

Figure 8: Dependence on degree of conversion for A, E_a, n_C and n_{O_2}. The parameter values were obtained by linear regression (least squares) over 5 wt.-% sub-conversion intervals, using nine isothermal experiments at three levels of oxygen and three temperatures per oxygen level. The error bars mark the 95% confidence regions.

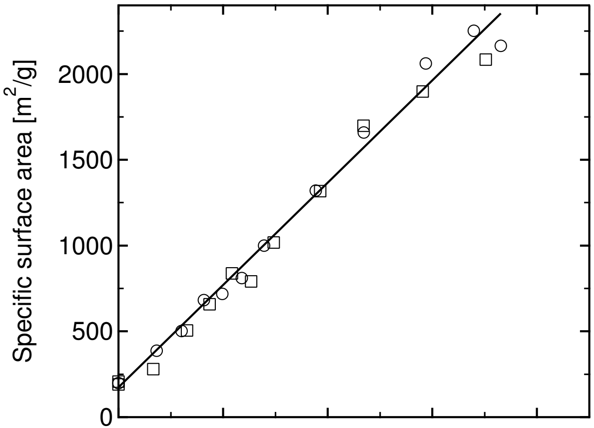

Figure 9: Specific BET surface area (the carbon mass is calculated from the outlet concentrations of CO and CO_2) of Printex U oxidized at 553±3°C using 8 vol.-% O_2 at different degrees of carbon conversion. The values are based on 4-5 measurements at relative pressures of nitrogen in the range 0.05-0.020 using a Micromeritics ASAP 2010. The samples were pretreated during two hours in vacuum at 250°C.

Controlled deposition of soot on cordierite substrates for kinetics analysis

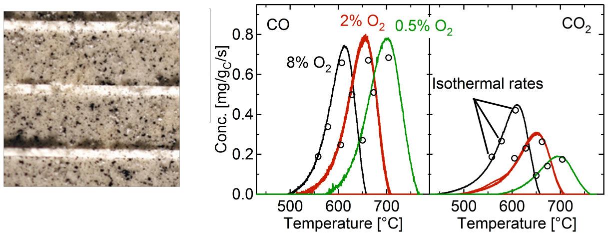

Figure 10: TOC figure